Biochemical and Biophysical Research Communications 423 (2012) 515–519

Contents lists available at SciVerse ScienceDirect

Biochemical and Biophysical Research Communications

journal homepage: www.elsevier.com/locate/ybbrc

The binding mechanism of eIF2β with its partner proteins, eIF5 and eIF2Bε

Zuoqi Gai [a], Yumie Kitagawa [a], Yoshikazu Tanaka [a,b], Nobutaka Shimizu [c], Keisuke Komoda [a,b], Isao Tanaka [a,b], Min Yao [a,b,*]

[a] Graduate School of Life Science, Hokkaido University, Sapporo 060-0810, Japan
[b] Faculty of Advanced Life Science, Hokkaido University, Sapporo 060-0810, Japan
[c] Structural Biology Research Center, Photon Factory, Institute of Materials Structure Science, High Energy Accelerator Research Organization (KEK), Tsukuba, Ibaraki 305-0801, Japan

ARTICLE INFO

Article history:
Received 21 May 2012
Available online 5 June 2012

Keywords:
Translation initiation
Intrinsically disordered domain
eIF2
eIF5
eIF2B

ABSTRACT

The eukaryotic translation initiation factor eIF2 delivers Met-tRNA$_i^{Met}$ to the ribosomal small subunit in GTP-bound form associated with eIF1, eIF1A, eIF3 and eIF5, and dissociates together with eIF5 as eIF5-eIF2-GDP complex from the ribosomal small subunit after formation of start codon–anticodon base pairing between Met-tRNA$_i^{Met}$ and mRNA. The inactive form eIF2-GDP is then exchanged for the active form eIF2-GTP by eIF2B for further initiation cycle. Previous studies showed that the C-terminal domains of eIF5 (eIF5-CTD) and eIF2Bε (eIF2Bε-CTD) have a common eIF2β-binding site for interacting with an N-terminal region of eIF2β (eIF2β-NTD). Here we have reconstructed the complexes of (eIF5-CTD)-(eIF2β-NTD) and (eIF2Bε-CTD)-(eIF2β-NTD) *in vitro*, and investigated binding mechanism by circular dichroism spectroscopy and small angle X-ray scattering in solution. The results showed the conformation of eIF2β-NTD was changed when bound to partner proteins, whereas the structures of eIF5-CTD and eIF2Bε-CTD were similar in both isolated and complex states. We propose that eIF2β-NTD works as an intrinsically disordered domain which is disorder in the isolated state, but folds into a definite structure when bound to its partner proteins. Such flexibility of eIF2β-NTD is expected to be responsible for its binding capability.

1. Introduction

Translation is a process of transforming the genetic information from mRNA into the functional proteins on the ribosome, and consists of three steps: initiation, elongation, and termination. Translational control is critical for gene regulation under conditions of nutrient deprivation and stress, development and differentiation, aging and disease in eukaryotic cells, and most regulations of translation are exerted at the translation initiation step [1–3].

Eukaryotic translation initiation is a process involving the assembly of an elongation-competent 80S ribosome, in which the start codon–anticodon is base-paired between Met-tRNA$_i^{Met}$ and mRNA on the ribosome [4]. It is performed by initiation factors (eIFs) associated with Met-tRNA$_i^{Met}$, mRNA, and ribosome. The initiation factor eIF2 consisting of α-, β-, and γ-subunits, is a G protein (γ-subunit), which is active in GTP-bound form and inactive in GDP-bound form [5,6]. The eIF2 in GTP-bound form plays a pivotal role in delivering Met-tRNA$_i^{Met}$ to ribosomal 40S and forms the 43S ribosomal subunit comprised of the 40S subunit and multiple factor complex MFC (eIF2-GTP- (Met – tRNA$_i^{Met}$) ternary complex, eIF3, eIF1, eIF1A and eIF5) [7]. This 43S pre-initiation complex is attached to the 5′ proximal region of mRNA to form ribosomal 48S, and scans mRNA in the 5′ to 3′ direction to search for the start codon [4]. After MFC binds to the 40S ribosomal subunit, the GTP on eIF2 is hydrolyzed to GDP, which is stimulated by the GTPase activator protein (GAP) eIF5 [8,9]. When the codon–anticodon base-pairing between Met-tRNA$_i^{Met}$ and mRNA is formed, eIF2-GDP and inorganic phosphate are released from ribosomal 48S [10]. It has been shown that eIF5 and eIF2 are released from the ribosome together in the form of eIF5-eIF2-GDP complex [11–14]. Then, the 48S complex binds to 60S to form the 80S ribosome, and then the elongation of protein synthesis is started. The released eIF2-GDP is inactive, and it must be exchanged to eIF2-GTP for further rounds of initiation. This reactivation is achieved by the guanine nucleotide exchange factor (GEF) eIF2B, which is a hetero-pentameric complex consisting of α, β, γ, δ, and ε subunits [6,15].

As described above, eIF2 binds to different target proteins at different reaction stages of the translation initiation. At the beginning of the initiation process (MFC formation), of the three subunits of eIF2, eIF2β is involved in direct binding to eIF1, eIF5, and eIF3, and mutations in eIF2β destabilize these interactions [6,16–18]. The C-terminal domain of eIF2β containing a C2–C2 Zinc binding motif is conserved in archaea and eukaryotes, whereas the N-terminal domain (eIF2β-NTD) is only conserved in eukaryotes [19–21]. Previous studies have shown that three lysine-rich segments (K-boxes) of eIF2β-NTD interact with two aromatic/acidic regions

* Corresponding author at: Graduate School of Life Science, Hokkaido University, Sapporo 060-0810, Japan. Fax: +81 11 706 4481.
E-mail address: yao@castor.sci.hokudai.ac.jp (M. Yao).

0006-291X/$ - see front matter © 2012 Elsevier Inc. All rights reserved.
http://dx.doi.org/10.1016/j.bbrc.2012.05.155

called AA box in the C-terminus of eIF5 (eIF5-CTD) [18,22]. In addition, the N-terminal domain of eIF5 (eIF5-NTD) interacts with the G domain of eIF2γ and functions as a GAP [23,24].

On the other hand, when eIF2B reactivates eIF2 by removing GDP and promoting association of GTP [6], the C-terminal domain of eIF2Bε (eIF2Bε-CTD) mediates the interaction between eIF2B subunits and promotes the changing of GDP for GTP bound with eIF2γ. Similar to eIF5-CTD, eIF2Bε-CTD also contains two AA boxes, which interact with K-boxes of eIF2β-NTD [25] (Supplementary Fig. S1A). The structures of eIF5-CTD (PDB ID: 2FUL) and eIF2Bε-CTD (PDB ID: 1PAQ) show that both eIF5-CTD and eIF2Bε-CTD have helical structures and AA boxes are contained in four C-terminal helices [26,27]. Structural comparison showed that eIF5-CTD and eIF2Bε-CTD have very similar secondary structures and topologies (α1–α9) but with different orientations in tertiary structure (Supplementary Fig. S1B). The surfaces of the four C-terminal helices in eIF5-CTD and eIF2Bε-CTD are also different (Supplementary Fig. S1C and D). Considering these results, it is suggested that eIF5-CTD and eIF2Bε-CTD may bind to eIF2β-NTD in different ways and/or with different affinities [27]. It has also been proposed that eIF5-eIF2 complex antagonizes guanine nucleotide exchange, enabling coordinated regulation of translation initiation based on the results of *in vivo* overexpression experiments [14]. However, it still remains to be elucidated how eIF2β binds to different target proteins eIF5 and eIF2Bε with the same binding site.

To address this problem, we studied the interaction mechanism of eIF2β-NTD with eIF5-CTD and eIF2Bε-CTD by analyzing the conformational changes of those proteins in both isolated and complex states. The circular dichroism (CD) spectroscopy and small angle X-ray scattering (SAXS) were used to examine the structures of eIF2β-NTD, eIF5-CTD, eIF2Bε-CTD, (eIF5-CTD)-(eIF2β-NTD), and (eIF2Bε-CTD)-(eIF2β-NTD). The results of current study showed that eIF2β-NTD is unstructured in isolated state and the conformation was changed when bound to partner proteins, whereas the structures of eIF5-CTD and eIF2Bε-CTD were similar in both isolated and complex states. The high flexibility of eIF2β-NTD is an advantage for structural changes according to further recognizing and binding with different proteins. Based on these results, we propose the manner of binding between eIF2β-NTD and both eIF5-CTD and eIF2Bε-CTD, and discuss the role of eIF2β-NTD as a part of eIF2.

2. Materials and methods

2.1. Protein expression and purification

The genes encoding eIF2β-NTD (1–124 aa, MW = 13,171 Da), eIF5-CTD (241–405 aa, MW = 18,967 Da) and eIF2Bε-CTD (538–712 aa, MW = 20,664 Da) of *Saccharomyces cerevisiae* with a hexahistidine (His_6) tag and a thrombin cleavage sequence at the N-terminus were individually cloned into the expression vector pET-28a fused with a D-box (ATGAATCATAAA). For overexpression, each resulting plasmid of eIF2β-NTD, eIF5-CTD, and eIF2Bε-CTD was transformed into *Escherichia coli* strain B834(DE) + pRARE2 by electroporation. The transformed cells were cultivated in Luria–Bertani (LB) containing 25 μg/mL kanamycin and 34 μg/mL chloramphenicol, and cultivated at 37 °C until the optical density at 600 nm (OD_{600}) reached about 0.6. After adding isopropyl β-d-1-thiogalactopyranoside (IPTG) to a final concentration of 0.5 mM, the cultures were incubated at 25 °C for an additional 16 h. The cells were harvested by centrifugation at 4500 × *g* under 4 °C for 25 min, and then washed in lysis-buffer (50 mM Tris–HCl, pH 8.0, 50 mM NaCl, 1 mM EDTA). The washed cells were collected by centrifugation at 6000× *g* under 4 °C for 15 min.

Recombinant eIF2β-NTD, eIF5-CTD, and eIF2Bε-CTD were purified separately using similar procedures as described in Supplementary methods. To reconstruct (eIF5-CTD)-(eIF2β-NTD) complex, purified eIF2β-NTD and eIF5-CTD were mixed in a molar ratio of 1:1 in the buffer (20 mM HEPES, pH 7.5, 10% glycerol, and 1 mM DTT) and incubated at room temperature for 30 min. The mixed sample was purified using a Superdex 75 16/60 gel-filtration column. The (eIF2Bε-CTD)-(eIF2β-NTD) complex was obtained using the same protocol.

2.2. Circular dichroism (CD) spectroscopy

The CD spectra were recorded on a J800 spectropolarimeter (Japan, Spectroscopic Company) under an atmosphere of N_2 at room temperature in a quartz cell with a path length of 2 mm. The samples of purified eIF2β-NTD, eIF5-CTD, eIF2Bε-CTD, (eIF5-CTD)-(eIF2β-NTD), and (eIF2Bε-CTD)-(eIF2β-NTD) were dialyzed in 10 mM sodium phosphate buffer at pH 7.5, 4 °C overnight before measurement. The CD spectra were obtained from a wavelength region of 190–300 nm by taking the average of four scans. The molar ellipticity per residues was calculated by $(\theta) = \theta / (10 n_* c_* l)$. Here, θ is the CD signal in mdeg, n is the number of residues, c is the concentration in mol L^{-1}, and l is the length of the cuvette path (cm). The concentrations of samples were measured using a Quant-iT™ Protein Kit (Invitrogen) three times, and the average values were applied to calculate molar ellipticity per residue. The CD spectra were analyzed using K2D2 online software package in order to estimate the occupancies of secondary structures [28].

2.3. Small-angle X-ray scattering (SAXS)

For SAXS measurement, the purified eIF2β-NTD, eIF5-CTD, eIF2Bε-CTD, (eIF5-CTD)-(eIF2β-NTD), and (eIF2Bε-CTD)-(eIF2β-NTD) were dialyzed against each buffer system (20 mM HEPES, pH 7.5, 30–100 mM NaCl, 5–10% Glycerol, and 1 mM DTT) at 4 °C overnight. In order to make samples avoid aggregation throughout the SAXS measurement, these buffer systems were optimized, and the final condition of buffer consisted of 20 mM HEPES pH 7.5, 30 mM NaCl, 10% Glycerol and 1 mM DTT. All samples were concentrated to around 6.0 mg/mL firstly, and the concentration of each sample (1.0–5.0 mg/mL) for SAXS measurement was also optimized for Guinier analysis.

The conditions of SAXS measurements were optimized at the beamline BL45, SPring-8 (Harima, Japan) [29], and final SAXS data collection was carried out at the beamline BL-10C, Photon Factory (Tsukuba, Japan) [30]. A wavelength of 1.488 Å was used, and the specimen-to-detector distance was 2034 mm calibrated with silver behenate. The exposure time was determined to be 10 min without aggregation caused by X-ray damage, and the temperature of the sample cell was maintained at 20 °C. The scattering images were recorded on an imaging plate detector (R-AXIS VII; Rigaku), and each two-dimensional scattering image was circularly averaged to convert the one-dimensional scattering intensity data. The radius of gyration R_g and the scattering intensity $I(0)$ were obtained by Guinier approximation in the small angle region:

$$I(Q) \cong I(0) \exp(-R_g^2/3 \times Q^2)$$

where $Q = 4\pi\sin\theta/\lambda$ is the amplitude of the scattering vector, $I(Q)$ is the scattering intensity at Q, 2θ is the scattering angle, λ is the wavelength of the X-rays, and $I(0)$ is the scattering intensity at $Q = 0$ [31]. As the slope and y-intersection of Ln $I(Q)$ vs. Q^2 (Guinier Plot) give $-{R_g}^2/3$ and Ln $I(0)$, respectively, R_g and $I(0)$, which is correlated with the total mass of the scatter, can be calculated based on the concentration (c) of each sample. Therefore, the intrinsic values of R_g and $I(0)/c$ were obtained by extrapolation to a concentration of zero to exclude the effect of sample concentration. The molecular weight of the sample can be estimated from $I(0)/c$ based on the

$I(0)/c$ value ($I(0)_{ref}/c_{ref}$) of a reference protein with a known MW. In this study, Ovalbumin (MW = 45 kDa) solutions in all types of buffer and at various concentrations (1.0–5.0 mg/mL) were measured as references. The values of R_g were estimated using the program Igor Pro ver. 6.22 J (http://www.wavemetrics.com) with a linear function of regression analysis, and the theoretical R_g values of eIF5-CTD and eIF2Bε-CTD were calculated with the program CRYSOL using crystal structures (PDB ID: 2FUL, PDB ID: 1PAQ) [32]. MWs were derived from Guinier analysis based on the $I(0)_{ref}/c_{ref}$ of ovalbumin solution. The asymptotic standard errors are shown in parentheses. Each R_g at the concentration of zero and the MW value were estimated from scattering profiles in a specific Q range ($Q \times R_g < 1.3$) by Guinier analysis, and are summarized in Supplementary Table S1. The scattering profiles by Kratky plot $I(Q) \times Q^2$ vs. Q were calculated to identify the structure state of these proteins in solution [33,34].

3. Results

3.1. Reconstructing the (eIF5-CTD)-(eIF2β-NTD) and (eIF2Bε-CTD)-(eIF2β-NTD) complex

The (eIF5-CTD)-(eIF2β-NTD) and (eIF2Bε-CTD)-(eIF2β-NTD) complexes were reconstructed using purified eIF2β-NTD, eIF5-CTD, and eIF2Bε-CTD. The purified (eIF5-CTD)-(eIF2β-NTD) and (eIF2Bε-CTD)-(eIF2β-NTD) complexes are shown in Fig. 1. Although there was no adsorption for eIF2β-NTD at a wavelength of 280 nm as eIF2β-NTD contains neither tyrosine nor tryptophan residues, peaks at a wavelength of 280 nm on the gel filtration plot were clearly shifted when either eIF5-CTD or eIF2Bε-CTD formed a complex with eIF2β-NTD (Fig. 1A and B), suggesting that both (eIF5-CTD)-(eIF2β-NTD) and (eIF2Bε-CTD)-(eIF2β-NTD) were formed by mixing purified eIF2β-NTD, eIF5-CTD, and eIF2Bε-CTD *in vitro*. Furthermore, while (eIF2Bε-CTD)-(eIF2β-NTD) could be confirmed clearly on SDS–PAGE (Supplementary Fig. S2A, lane 7) and TOF MASS (Supplementary Fig. S2B, E, F), (eIF5-CTD)-(eIF2β-NTD) could only be detected by TOF MASS (Supplementary Fig. S2B, C, D), as the bands of eIF5-CTD and eIF2β-NTD were located at the same position on SDS–PAGE (Supplementary Fig. S2B, lane 6).

3.2. Conformational changes in eIF2β-NTD upon binding to partner proteins

The CD spectroscopy was used to analyze the conformational changes that may occur upon binding of eIF2β-NTD to its partner proteins, eIF5-CTD and eIF2Bε-CTD. The CD spectra of eIF2β-NTD, eIF5-CTD, eIF2Bε-CTD, (eIF5-CTD)-(eIF2β-NTD), and (eIF2Bε-CTD)-(eIF2β-NTD) are shown in Fig. 2A and B. The CD spectra of both eIF5-CTD and eIF2Bε-CTD showed two negative peaks at 208 and 222 nm, suggesting that they are typical helical structures. Based on the CD spectra, the occupancies of α-helix of two proteins were estimated to be 84 and 76%, respectively. Although not accurately quantitative of the estimation, these results were consistent with that of the reported crystal structures of eIF5-CTD and eIF2Bε-CTD, both of which consist of only α-helices and the calculated occupancies of α-helix are about 82 and 73% with the remainder random coil, respectively. In contrast, the spectrum of eIF2β-NTD showed a typical random coil plot with minimum ellipticity near 200 nm, and calculation given over 70% random coil.

Interestingly, although the spectrum of eIF2β-NTD showed a typical random coil plot, the CD spectra of both (eIF5-CTD)-(eIF2β-NTD) and (eIF2Bε-CTD)-(eIF2β-NTD) complexes also showed typical helical structural sharps similar to those of eIF5-CTD and eIF2Bε-CTD, respectively. While the spectrum of (eIF2Bε-CTD)-(eIF2β-NTD) was very similar to that of isolated (eIF2Bε-CTD), the plot difference between (eIF5-CTD)-(eIF2β-NTD) and (eIF5-CTD) suggested the difference of helical percentage. Moreover, the estimations of these data also showed that α-helix occupancies of (eIF2Bε-CTD)-(eIF2β-NTD) was similar to that of eIF2Bε-CTD, while the α-helical percentage of (eIF5-CTD)-(eIF2β-NTD) was increased (more than 80%), suggesting that (eIF5-CTD)-(eIF2β-NTD) may be more compact than (eIF5-CTD). Taken all results together, it was suggested that eIF2β-NTD is a disordered domain in isolated situation, but may form helical structure when it binds to eIF5-CTD or eIF2Bε-CTD.

3.3. SAXS analysis of eIF2β-NTD, eIF5-CTD, eIF2Bε-CTD and their complexes

To elucidate the structures of eIF2β-NTD, eIF5-CTD, eIF2Bε-CTD, (eIF5-CTD)-(eIF2β-NTD), and (eIF2Bε-CTD)-(eIF2β-NTD) in solution, SAXS experiments were performed using synchrotron radiation. Table S1 in Supplementary summarizes the radius of gyration R_g at the concentration of zero and MW values estimated from scattering profiles in a specific Q range by Guinier analysis. The estimated MWs of all samples indicated that eIF2β-NTD, eIF5-CTD, eIF2Bε-CTD were monomeric in solution, and two complexes of (eIF5-CTD)-(eIF2β-NTD) and (eIF2Bε-CTD)-(eIF2β-NTD) were also single complexed molecules in solution. While the obtained R_g values of eIF2Bε-CTD from SAXS data were compared with the calculation volumes estimated from the crystal structure, the R_g value of eIF5-CTD was larger than that of the crystal structure, suggesting that eIF5-CTD shows marked fluctuation in solution. On the other hand, the R_g values of both (eIF5-CTD)-(eIF2β-NTD) and (eIF2Bε-CTD)-(eIF2β-NTD) complex were similar

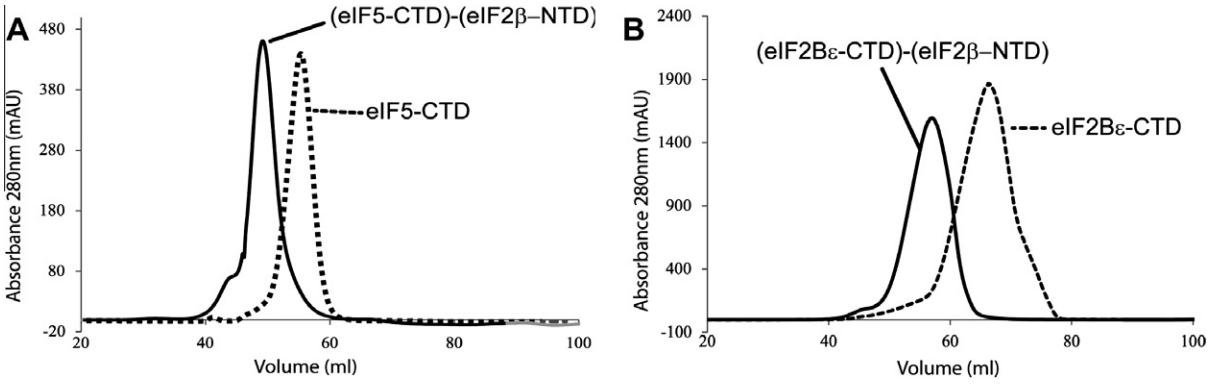

Fig. 1. Reconstruction of complexes. The reconstructed complexes of (eIF5-CTD)-(eIF2β-NTD) (A) and (eIF2Bε-CTD)-(eIF2β-NTD) (B), were purified by gel filtration column chromatography. (For interpretation of the references to colour in this figure legend, the reader is referred to the web version of this article.)

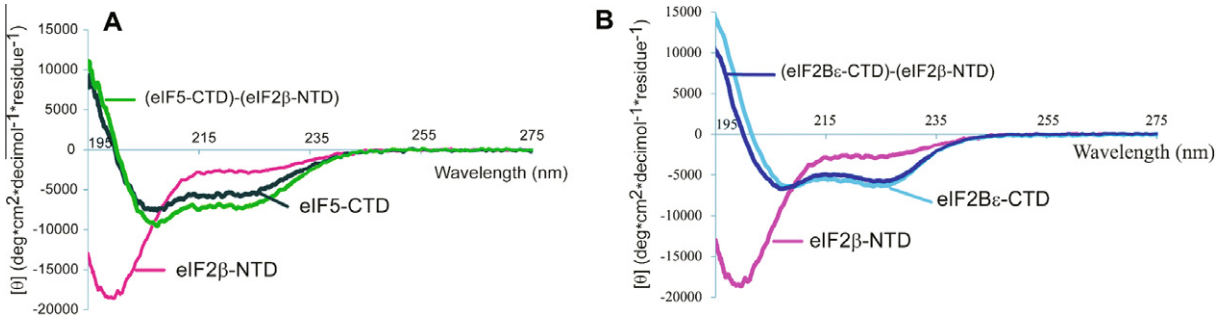

Fig. 2. CD spectra. A. CD spectra of eIF2β-NTD (purple), eIF5-CTD (yellow), and (eIF5-CTD)-(eIF2β-NTD) complex (green). (B). CD spectra of eIF2β-NTD (purple), eIF2Bε-CTD (blue) and (eIF2Bε-CTD)-(eIF2β-NTD) complex (cyan).

to that of eIF2β-NTD, indicating that eIF2β-NTD may be less flexible in both complexes than in isolated situation.

The Kratky plot, $I(Q) \times Q^2$ vs. Q plot of SAXS data, is a useful expression of the structural characteristics for protein folding studies. Therefore, Kratky analyses of all samples were performed using the measured scattering curve to obtain information on the folding status (Fig. 3A and B). The Kratky plot of eIF2β-NTD showed a plateau shape in the region of $Q > 0.08$. This kind of shape clearly indicated a random-coiled structure. In contrast, Kratky plots of both (eIF2Bε-CTD)-(eIF2β-NTD) and (eIF5-CTD)-(eIF2β-NTD) complexes had a well-defined peak around $Q = 0.05$. In comparison with the Kratky plots of eIF5-CTD and eIF2Bε-CTD, the peaks of the two complexes were also shifted to lower Q, corresponding to larger R_g. These Kratky plots suggested that isolated eIF2β-NTD was unfolded, and formed a structure when it bound to eIF5-CTD or eIF2Bε-CTD. Moreover, in comparison with the Kratky plot of (eIF5-CTD), the (eIF5-CTD)-(eIF2β-NTD) complex was more compacted than isolated eIF5-CTD.

4. Discussion

During the process of translation initiation, the eIF2β-NTD plays an important role as a binding domain in interacting with various initiation factors, such as eIF1, eIF3, eIF5, and eIF2Bε in different reaction stages. Interestingly, among those interactions, the eIF2β-NTD binds to the C-terminus of eIF5 (eIF5-CTD) or eIF2Bε (eIF2Bε-CTD) with the same binding site. The characteristics of interacted residues between eIF2β-NTD and both eIF5-CTD and eIF2Bε-CTD were identified: both eIF5-CTD and eIF2Bε-CTD have the common regions of AA-boxes that interact with the same regions (K-boxes) of eIF2β-NTD (Supplementary Fig. S1). However, as shown in Supplementary Fig. S1, the structures of the C-terminal region including the AA-boxes in eIF5-CTD and eIF2Bε-CTD are different. As in our experiment of CD and SAXS, we found that eIF2β-NTD is highly unstructured in the isolated state but forms a structure when it binds to eIF5-CTD or eIF2Bε-CTD. Such eIF2β-NTD works as an intrinsically disordered domain. The disorder of eIF2β-NTD is expected to be responsible for its binding capability that recognizes and binds to different structural shapes and sequences of partner proteins by the same binding site.

It has been known that when the start codon is paired with its anticodon, eIF5-eIF2-GDP complex is released from ribosomes, and such inactive eIF2-GDP has to be exchanged for the active form of eIF2-GTP with the aid of eIF2B for the next round of initiation. eIF5, which has GDP dissociation inhibitor (GDI) activity [35,36], should dissociate from eIF5-eIF2-GDP complex, and eIF2B consequently binds to eIF2-GDP. In order to release eIF5, then binds to the eIF2Bε-CTD via the same regions, eIF2β-NTD should undergo structural changes. The unfolding situation of eIF2β-NTD in the isolated state is an advantage for structural changes according to further interaction with different proteins.

Based on discuss above, we propose a binding mechanism of eIF2β-NTD with different proteins in different stages of translation initiation (Fig. 4). eIF2β-NTD is an intrinsically disordered domain required for its function that recognizes and binds to the different proteins in the different reaction stages. The binding event of eIF5 to eIF2 induces eIF2β-NTD to form a structure that recognizes eIF5-CTD and binds strongly, aiding in the interaction between eIF2γ and eIF5. After eIF5 stimulates the hydrolysis of eIF2-GTP to eIF2-GDP, and the codon–anticodon base pairing between Met-tRNA$_i^{Met}$ and mRNA is formed, eIF5-eIF2-GDP and inorganic phosphate are released from the ribosome. As eIF2Bε-CTD has higher binding affinity with eIF2β-NTD than that of eIF5-CTD, eIF2B can replace eIF5 in eIF5-eIF2-GDP complex and form eIF2B-eIF2-GDP complex to reactivate eIF2 by exchanging GDP to GTP. In this stage, the formation of eIF2B-eIF2-GDP complex also induces structural changes in eIF2β-NTD to form a structure for bind-

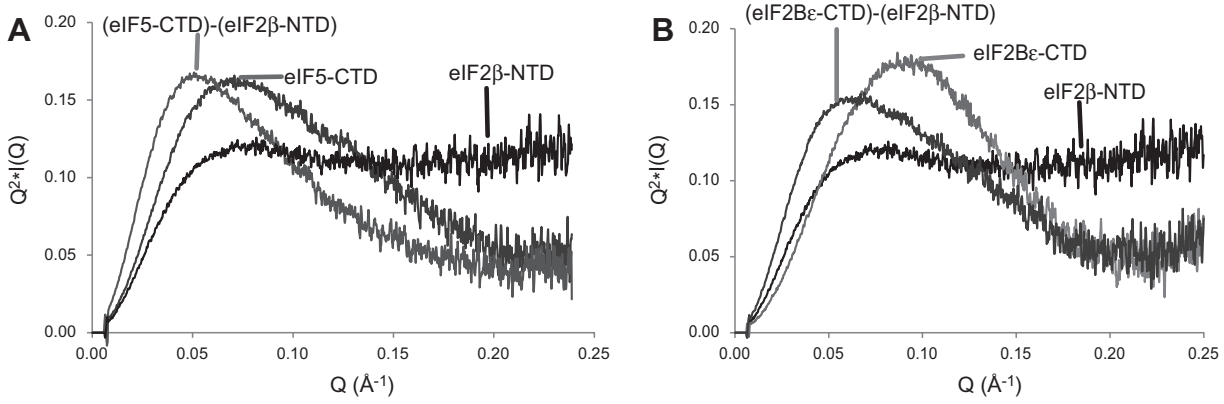

Fig. 3. Kratky analysis of SAXS. A Kratky plots of eIF2β-NTD, eIF5-CTD, and (eIF5-CTD)-(eIF2β-NTD) complex. B. Kratky plots of eIF2β-NTD, eIF2Bε-CTD, and (eIF2Bε-CTD)-(eIF2β-NTD) complex.

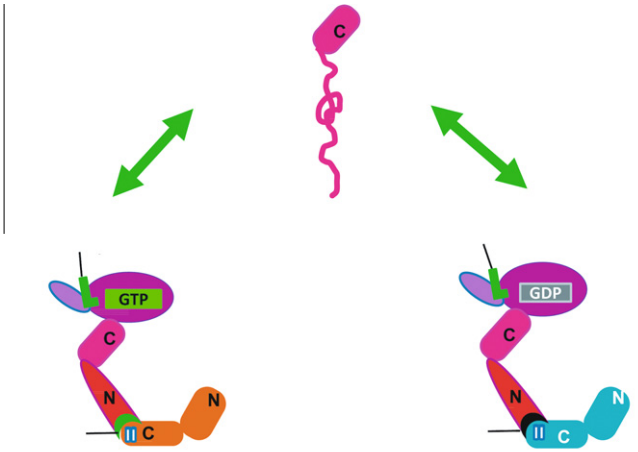

Fig. 4. A model of the binding manner of eIF2 with eIF5 and eIF2Bε. The left diagram shows eIF2-GTP interacted with eIF5 in the start-codon-scan stage. The right diagram shows inactive form eIF2-GDP interacted with eIF2Bε in the reactivation stage. N and C indicate the N-terminal and C-terminal domains, respectively.

ing to eIF2Bε-CTD. Moreover, when eIF5 or eIF2B dissociates, eIF2β-NTD should dynamically changes the structure into random coli. It will be necessary to elucidate the structures of eIF5-eIF2 and eIF2B-eIF2 to determine the detailed manner of recognition of eIF2 with its partner proteins eIF5 and eIF2B.

Acknowledgments

We thank Dr Masaaki Sokabe, Dr Toyoyuki Ose and Dr Takashi Matsui for their assistance in the current research. We also thank the staff of beamline BL45, SPring-8 of Japan for their help with SAXS data measurements. Zuoqi Gai was supported by the International Graduate Program for Research Pioneers in Life Sciences (IGP-RPLS). This work was supported by Grant-in-aid for Scientific Research (B) (No. 21370041 to M. Y) from the Ministry of Education, Culture, Sports, Science and Technology of Japan.

Appendix A. Supplementary data

Supplementary data associated with this article can be found, in the online version, at http://dx.doi.org/10.1016/j.bbrc.2012.05.155.

References

[1] G. Hernandez, M. Altmann, P. Lasko, Origins and evolution of the mechanisms regulating translation initiation in eukaryotes, Trends Biochem. Sci. 35 (2009) 63–73.
[2] N. Sonenberg, A.G. Hinnebusch, Regulation of translation initiation in eukaryotes: mechanisms and biological targets, Cell 136 (2009) 731–745.
[3] D. Silvera, S.C. Formenti, R.J. Schneider, Translational control in cancer, Nat. Rev. Cancer 10 (2010) 254–266.
[4] R.J. Jackson, C.U.T. Hellen, T.V. Pestova, The mechanism of eukaryotic translation initiation and principles of its regulation, Nat. Rev. Mol. Cell Biol. 11 (2010) 113–127.
[5] E.A. Stolboushkina, M.B. Garber, Eukaryotic type translation initiation factor 2: structure-functional aspects, Biochemistry (Moscow) 76 (2011) 283–294.
[6] S.S. Mohammad-Qureshi, M.D. Jennings, G.D. Pavitt, Clues to the mechanism of action of eIF2B, the guanine-nucleotide-exchange factor for translation initiation, Biochem. Soc. Trans. 36 (2008) 658–664.
[7] K. Asano, J. Clayton, A. Shalev, A.G. Hinnebusch, A multifactor complex of eukaryotic initiation factors, eIF1, eIF2, eIF3, eIF5, and initiator tRNA(Met) is an important translation initiation intermediate in vivo, Genes Dev. 14 (2000) 2534–2546.
[8] F.E.M. Paulin, L.E. Campbell, K. O'Brien, J. Loughlin, C.G. Proud, Eukaryotic translation initiation factor 5 (eIF5) acts as a classical GTPase-activator protein, Curr. Biol. 11 (2001) 55–59.
[9] J. Nika, S. Rippel, E.M. Hannig, Biochemical analysis of the eIF2βγ complex reveals a structural function for eIF2α in catalyzed nucleotide exchange, J. Biol. Chem. 276 (2001) 1051–1056.
[10] M.A. Algire, D. Maag, J.R. Lorsch, Pi release from eIF2, not GTP hydrolysis, is the step controlled by start-site selection during eukaryotic translation initiation, Mol. Cell 20 (2005) 251–262.
[11] A. Unbehaun, S.I. Borukhov, C.U.T. bHellen, T.V. Pestova, Release of initiation factors from 48S complexes during ribosomal subunit joining and the link between establishment of codon–anticodon base-pairing and hydrolysis of eIF2-bound GTP, Genes Dev. 18 (2004) 3078–3093.
[12] Y.N. Cheung, D. Maag, S.F. Mitchell, C.A. Fekete, M.A. Algire, J.E. Takacs, N. Shirokikh, T. Pestova, J.R. Lorsch, A.G. Hinnebusch, Dissociation of eIF1 from the 40S ribosomal subunit is a key step in start codon selection in vivo, Genes Dev. 21 (2007) 1217–1230.
[13] C.R. Singh, T. Udagawa, B. Lee, S. Wassink, H. He, Y. Yamamoto, J.T. Anderson, G.D. Pavitt, K. Asano, Change in nutritional status modulates the abundance of critical pre-initiation intermediate complexes during translation initiation in *vivo*, J. Mol. Biol. 370 (2007) 315–330.
[14] C.R. Singh, B. Lee, T. Udagawa, S.S. Mohammad-Qureshi, Y. Yamamoto, G.D. Pavitt, K. Asano, An eIF5/eIF2 complex antagonizes guanine nucleotide exchange by eIF2B during translation initiation, EMBO J. 25 (2006) 4537–4546.
[15] T.V. Pestova, C.U.T. Hellen, The structure and function of initiation factors in eukaryotic protein synthesis, Cell. Mol. Life Sci. 57 (2000) 651–674.
[16] M. Reibarkh, Y. Yamamoto, C.R. Singh, F. del Rio, A. Fahmy, B. Lee, R.E. Luna, M. Ii, G. Wagner, K. Asano, Eukaryotic initiation factor (eIF) 1 carries two distinct eIF5-binding faces important for multifactor assembly and AUG selection, J. Biol. Chem. 283 (2008) 1094–1103.
[17] L. Valasek, K.H. Nielsen, A.G. Hinnebusch, Direct eIF2-eIF3 contact in the multifactor complex is important for translation initiation *in vivo*, EMBO 21 (2002) 5886–5898.
[18] K. Asano, T. Krishnamoorthy, L. Phan, G.D. Pavitt, A.G. Hinnebusch, Conserved bipartite motifs in yeast eIF5 and eIF2Be, GTPase-activating and GDP-GTP exchange factors in translation initiation, mediate binding to their common substrate eIF2, EMBO J. 18 (1999) 1673–1688.
[19] M. Sokabe, M. Yao, N. Sakai, S. Toya, I. Tanaka, Structure of archaeal translational initiation factor 2βγ-GDP reveals significant conformational change of the β-subunit and switch 1 region, Proc. Natl. Acad. Sci. U. S. A. 103 (2006) 13016–13021.
[20] P. Gutierrez, M.J. Osborne, N. Siddiqui, J.F. Trempe, C. Arrowsmith, K. Gehring, Structure of the archaeal translation initiation factor aIF2β from methanobacterium thermoautotrophicum: implications for translation initiation, Protein Sci. 13 (2004) 659–667.
[21] J.P. Laurino, G.M. Thompson, E. Pacheco, B.A. Castilho, The β subunit of eukaryotic translation initiation factor 2 binds mRNA through the lysine repeats and a region comprising the C-2-C-2 motif, Mol. Cell. Biol. 19 (1999) 173–181.
[22] S. Das, T. Maiti, K. Das, U. Maitra, Specific interaction of eukaryotic translation initiation factor 5 (eIF5) with the b subunit of eIF2, J. Biol. Chem. 272 (1997) 31712–31718.
[23] M.R. Conte, G. Kelly, J. Babon, D. Sanfelice, J. Youell, S.J. Smerdon, C.G. Proud, Structure of the eukaryotic initiation factor (eIF) 5 reveals a fold common to several translation factors, Biochemistry 45 (2006) 4550–4558.
[24] P.V. Alone, T.E. Dever, Direct binding of translation initiation factor eIF2γ-G domain to its GTPase- activating and GDP-GTP exchange factors eIF5 and eIF2Bε, J. Biol. Chem. 281 (2006) 12636–12644.
[25] E.V. Koonin, Multidomain organization of eukaryotic guanine nucleotide exchange translation initiation factor eIF2B subunits revealed by analysis of conserved sequence motifs, Protein Sci. 4 (1995) 1608–1617.
[26] T. Boesen, S.S. Mohammad, G.D. Pavitt, G.R. Andersen, Structure of the catalytic fragment of translation initiation factor 2B and identification of a critically important catalytic residue, J. Biol. Chem. 279 (2004) 10584–10592.
[27] Z. Wei, Y. Xue, H. Xu, W. Gong, Crystal structure of the C-terminal domain of *S .cerevisiae* eIF5, J. Mol. Biol. 359 (2006) 1–9.
[28] C. Perez-Iratxeta, M.A. Andrade-Navarro, K2D2: estimation of protein secondary structure from circular dichroism spectra, BMC. Struct. Biol. 8 (2008) 25.
[29] T. Fujisawa, K. Inoue, T. Oka, H. Iwamoto, T. Uruga, T. Kumasaka, Y. Inoko, N. Yagi, M. Yamamoto, T. Ueki, Small-angle X-ray scattering station at the SPring-8 RIKEN beamline, J. Appl. Crystallogr. 33 (2000) 797–800.
[30] N. Igarashi, Y. Watanabe, Y. Shinohara, Y. Inoko, G. Matsuba, H. Okuda, T. Mori, K. Ito, Upgrade of the small angle X-ray scattering beamlines at the Photon Factory, J. Phys. Conf. Ser. 272 (2011) 012026.
[31] A. Guinier, G. Fournet, Small Angle X-ray Scattering, John-Wiley and Sons, New York, 1955.
[32] D. Svergun, C. Barberato, M.H.J. Koch, CRYSOL - a program to evaluate X-ray solution scattering of biological macromolecules from atomic coordinates, J. Appl. Crystallogr. 28 (1995) 768–773.
[33] M. Kataoka, I. Nishii, T. Fujisawa, T. Ueki, F. Tokunaga, Y. Goto, Structural characterization of the molten globule and native states of apomyoglobin by solution X-ray scattering, J. Mol. Biol. 249 (1995) 215–228.
[34] O. Glatter, O. Kratky, Small Angle X-ray Scattering, Academic Press, New York, 1982.
[35] M.D. Jennings, G.D. Pavitt, EIF5 has GDI activity necessary for translational control by eIF2 phosphorylation, Nature 465 (1982) 378–381.
[36] M.D. Jennings, G.D. Pavitt, eIF5 is a dual function GAP and GDI for eukaryotic translational control, Small Gtpases 1 (2011) 118–123.